PAPER

Beta decay of ^{66}Mn to the N = 40 nucleus ^{66}Fe

To cite this article: B Olaizola *et al* 2017 *J. Phys. G: Nucl. Part. Phys.* **44** 125103

View the article online for updates and enhancements.

Related content

Beta decay of ^{66}Mn to the $N = 40$ nucleus ^{66}Fe

B Olaizola[1,13] , **L M Fraile**[1] , **H Mach**[1,2,14], **A Poves**[3] ,
A Aprahamian[4], **J A Briz**[5,15], **J Cal-González**[1,16], **D Ghiţa**[6],
U Köster[7], **W Kurcewicz**[8], **S R Lesher**[4,9], **D Pauwels**[10],
E Picado[1,11], **D Radulov**[10], **G S Simpson**[12] and **J M Udías**[1]

[1] Grupo de Física Nuclear y UPARCOS, Universidad Complutense—CEI Moncloa, E-28040 Madrid, Spain
[2] BP1, NCBJ—National Center for Nuclear Research, Otwock, Poland
[3] Departamento de Física Teórica e IFT-UAM/CSIC, Universidad Autónoma de Madrid, E-28049 Madrid, Spain
[4] Department of Physics, University of Notre Dame, Notre Dame, IN 46556, United States of America
[5] Instituto de Estructura de la Materia, CSIC, E-28006 Madrid, Spain
[6] Horia Hulubei National Institute of Physics and Nuclear Engineering, Bucharest, Romania
[7] Institut Laue-Langevin, B.P. 156, F-38042 Grenoble Cedex 9, France
[8] Faculty of Physics, University of Warsaw, Pasteura 5, PL 02-093 Warsaw, Poland
[9] Department of Physics, University of Wisconsin—La Crosse, La Crosse, WI 54601, United States of America
[10] K.U. Leuven, IKS, Celestijnenlaan 200 D, B-3001 Leuven, Belgium
[11] Sección de Radiaciones, Departamento de Física, Universidad Nacional, Heredia, Costa Rica
[12] LPSC, Université Joseph Fourier Grenoble 1, CNRS/IN2P3, Institut National Polytechnique de Grenoble, F-38026 Grenoble Cedex, France

E-mail: bruno.olaizola@ucm.es

CrossMark

Abstract

The low energy structure of ^{66}Fe was studied by means of γ- and fast-timing spectroscopy at the ISOLDE/CERN facility. The level scheme of ^{66}Fe populated following the β^- decay of ^{66}Mn was established. It confirms and further expands the level scheme from recent publications. The β-delayed

neutron emission branch was measured and γ rays in ^{65}Fe were observed following the β–n decay for the first time. The half lives of the 2_1^+ state and four other states of ^{66}Fe were measured using the advanced time-delayed $\beta\gamma\gamma(t)$ method. These results are compared with large-scale shell-model calculations based on the Lenzi–Nowacki–Poves–Sieja interaction. The β-decay of ^{66}Mn to ^{66}Fe has been calculated as well, and log(ft) values derived. Spin and parity assignments are proposed based on the experimental information and the new calculations.

(Some figures may appear in colour only in the online journal)

1. Introduction

Although ^{68}Ni ($Z = 28$, $N = 40$) shows some of the characteristics of a doubly magic nucleus, such as a high E(2^+) of more than 2 MeV [1] and a small B(E2;$2_1^+ \rightarrow 0_1^+$) value of 3.2 W.u. [2], mass measurements have shown that the oscillator gap at $N = 40$ is weak for ^{68}Ni [3], and imply that the small B(E2) value does not necessarily indicate a sub-shell closure. In addition, the first excited state at 1.6 MeV has 0^+ spin-parity, and it has been suggested that this level and the 2_1^+ state are members of an oblate structure [4–6]. The presence of low-lying 0^+ states has been interpreted as proof of shape coexistence in the region [6–8].

Nuclei around ^{68}Ni have motivated many recent experimental and theoretical studies, aimed at the understanding of the nuclear structure in this region with a large neutron excess. The erosion of the $N = 40$ gap can be seen as soon as 2 or 4 protons are removed from ^{68}Ni. The development of collectivity has been observed in the even–even Fe and Cr isotopes around $N = 40$ by the lowering of the 2_1^+ state energies and the increase of the B(E2;$2_1^+ \rightarrow 0_1^+$) transition rates. For the isotopes ^{66,68}Fe the 2_1^+ energies are 573 keV [9] and 521 keV [10, 11], respectively. For ^{66}Fe the B(E2) value has been measured twice, 21(2) W.u. by Rother *et al* [12] from the $\tau = 39.4(40)$ ps lifetime using the recoil distance Doppler-shift technique, and 18(2) W.u. by Coulomb excitation by Crawford *et al* [11]. For ^{68}Fe a transition rate of 22(3) W.u. was reported in [11]. The $N = 40$ nucleus ^{64}Cr, which in a single-particle interpretation of the shell model has half occupation of the $f_{7/2}$ proton orbit ($Z = 24$), has an even lower 2_1^+ level at 420 keV [13] and an enhanced E2 transition to the ground state with B(E2;$2_1^+ \rightarrow 0_1^+$) = 21(5) W.u. [11]. These facts point to the departure from magicity and the weakening of the $N = 40$ sub-shell gap in the region below ^{68}Ni.

The enhancement of quadrupole collectivity is understood as the result of the promotion of neutron pairs across the $N = 40$ sub-shell to the $\nu 0g_{9/2}$ and $\nu 1d_{5/2}$ orbitals, which are members of a variant of Elliot's SU3 symmetry due to their close energy [14]. The important role of the $\nu 0g_{9/2}$ orbit is revealed by the decreasing excitation energy of the $9/2^+$ isomers in the odd Fe isotopes [15–18]. When moving away from Ni ($Z = 28$) to Fe ($Z = 26$) and then Cr ($Z = 24$), thus taking protons out from the $\pi 0f_{7/2}$ orbital, the attractive particle–particle tensor interaction is reduced (since the particles in the $0f_{7/2}$ and $0f_{5/2}$ are anti-aligned), pushing the neutron $\nu 0f_{5/2}$ orbital to higher energy [19]. At the same time the excitation of neutrons to the intruder positive parity orbital $\nu 0g_{9/2}$ becomes more and more relevant. The attractive proton–neutron interaction between proton holes in the $\pi 0f_{7/2}$ orbital and neutrons in the $\nu 0g_{9/2}$ and $\nu 1d_{5/2}$ orbitals drags these neutron single-particle levels to lower energies. As a result the $N = 40$ gap is strongly diminished.

Large-scale shell-model calculations using the LNPS effective interaction have succeeded in reproducing both the excitation energies of neutrons to the $\nu 0g_{9/2}$ and $\nu 0f_{5/2}$ orbitals and the transition rates from the resulting states [20]. The calculations use ^{48}Ca as a core and the *pf* shell for protons and the $1p_{3/2}$, $1p_{1/2}$, $0f_{5/2}$, $0g_{9/2}$ and $1d_{5/2}$ orbitals for neutrons. A strong quadrupole deformation, coming nearer the rotational regime, is predicted for Cr isotopes. Multiparticle–multihole configurations play a key role in the ground state wave function with as many as four neutrons in the intruder $g_{9/2}$ and $d_{5/2}$ orbitals from the upper oscillator shell. Despite the success of the LNPS interaction in reproducing most of the experimental results, the prediction of maximum collectivity in the region occurs for ^{64}Cr and its onset at $N = 40$ for the Fe isotopes [20]. However, experiments show that ^{64}Fe has a higher B(E2; $2_1^+ \rightarrow 0_1^+$) than ^{66}Fe, and even than ^{64}Cr, albeit in the latter case the difference is well within one standard deviation [12, 21]. The confirmation of these experimental results is vital to understand the evolution of nuclear structure in the region and the interplay between single particle states and collectivity.

The first spectroscopic information on ^{66}Fe came from the identification of the 2_1^+ state at 573.4 keV by Hannawald *et al* [9]. They also observed a γ transition of 840.5 keV in coincidence with the 573.4 keV decay, and tentatively assigned a spin-parity of (4^+) to the 1414 keV level. The $2_1^+ \rightarrow 0_1^+$ transition was also observed at 574.7(10) keV in [16]. In one- and two-proton knockout reaction experiment from cobalt and nickel, Adrich *et al* [10] observed a γ ray of 832(9) keV depopulating a level at 1407 keV in ^{66}Fe, which was ascribed as $J^\pi = 4^+$, in contrast to the previous assignment of this spin to the level at 1414 keV. They also observed transitions of 957(10) and 1310(15) keV, but they could not place them in the level scheme. The multipolarity of the transitions was not assigned either. Later, Fioretto *et al* [22] populated excited ^{66}Fe levels in a ^{64}Ni + ^{238}U reaction at 400 MeV. The $2^+ \rightarrow 0^+$ 574 keV, $4^+ \rightarrow 2^+$ 834 keV and $6^+ \rightarrow 4^+$ 957 keV transitions were observed. Liddick *et al* published a ^{66}Mn β-decay study [23] where the low-energy level scheme of ^{66}Fe was constructed including a total of 17 γ-rays and 9 levels and they reported a β-delayed neutron emission branch value of $P_n = 4(1)\%$.

In this paper we report on the investigation of the low energy structure of ^{66}Fe, populated in the β decay of ^{66}Mn. Our study via $\gamma\gamma$ and fast-timing spectroscopy adds 10 new transitions, discards two tentative ones and incorporates 7 new states up to 3.6 MeV to the available level scheme by Liddick *et al* [23]. The direct β-feeding to the ground state and the P_n value have also been measured. Lifetimes and lifetime limits of some of the lower energy levels have been obtained using the advanced time-delayed (ATD) $\beta\gamma\gamma(t)$ method, including the previously known first 2^+ state. Tentative spin-parity assignments are proposed. Shell-model calculations based on the LNPS interaction have been performed for the ^{66}Mn β-decay and ^{66}Fe excitation structure, and compared to the experimental results.

2. Experimental results

The $A = 66$ data were collected for 30 h at the ISOLDE/CERN facility. The isotopes were created by protons of 1.4 GeV impinging on an UC_X target. The protons come from the CERN PS Booster in pulses spaced by multiples of 1.2 s. The Mn atoms were released from the target and selectively ionized by the resonant ionization laser ion source. The ions were then accelerated to 30 kV and those with $A = 66$ were selected in mass-to-charge ratio by the general purpose separator and transported to the experimental station. Due to its low ionization potential, Ga atoms were surface-ionized and ^{66}Ga was present as a contaminant in the beam. Owing to the long ^{66}Ga half-life, $T_{1/2} = 9.49(3)$ h, the ^{66}Ga activity could be
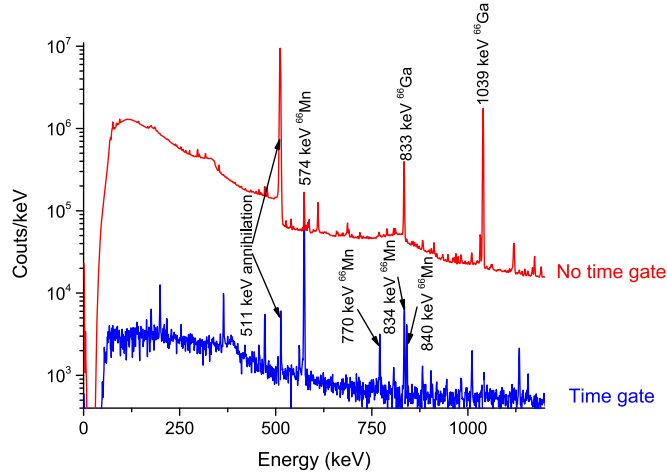
Figure 1. *Red, higher statistics*: singles HPGe energy spectrum with no time condition. The ^{66}Ga activity is clearly dominant. *Blue, lower statistics:* singles HPGe energy spectrum with a time selection from proton impact on target to enhance ^{66}Mn activity and long-lived ^{66}Ga activity subtracted. The ^{66}Ga lines are completely suppressed with no significant loss of ^{66}Mn decay.

subtracted and the ^{66}Mn decay was further enhanced by selecting a time window of 10–600 ms after proton impact (see figure 1).

The beam collection point was surrounded by five detectors in very close geometry. A fast-timing NE111A plastic scintillator for β particles was positioned immediately after the deposition point. Two LaBr$_3$(Ce) were used as fast timing γ-ray detectors. They had the shape of truncated cones (38.1 mm in height, 38.1 mm diameter at the bottom and 25.4 mm diameter at the entrance window), and were coupled to Photonis XP20D0 photomultipliers. Two high purity germanium (HPGe) detectors with relative efficiencies of 60% were also included. The experimental station and the data collection were optimized for the application of the ATD $\beta\gamma\gamma(t)$ method described in [24–26]. This experiment was part of a wider campaign that aimed to systematically study the nuclear chart below ^{68}Ni. Further details on the campaign, including the experimental setup and the data processing, can be found in [17, 18, 27, 28].

2.1. ^{66}Fe level scheme

The assignment of γ rays to ^{66}Fe was based on their parent decay half-life and coincidence relations with previously assigned transitions. Our data were not optimized to measure the ^{66}Mn half-life, but to maximize the amount of ^{66}Mn ions arriving to the experimental area. Nonetheless we have obtained a value of $T_{1/2} = 70(15)$ ms (see figure 2) for the ^{66}Mn half-life, which is consistent with the published values of $T_{1/2} = 65(2)$ ms [29] and the more recent 60(3) ms [23], and allows to unambiguously distinguish the ^{66}Mn decay from the other decays in the chain.

Figure 3 shows the HPGe–HPGe coincidences gated on the 573.5 keV γ ray. Most of the transitions observed in ^{66}Fe are in coincidence with this one. Only the 1881.2, 2874.3 and 3284.7 keV transitions were not observed in this coincidence spectrum, and thus were placed in the scheme based on its mother nucleus half-life (all below 100 ms, but with low precision) and the fact that they fitted the energies of other independently established levels. Two other high-energy γ rays with not enough statistics to be observed in $\gamma\gamma$ coincidences, but with a
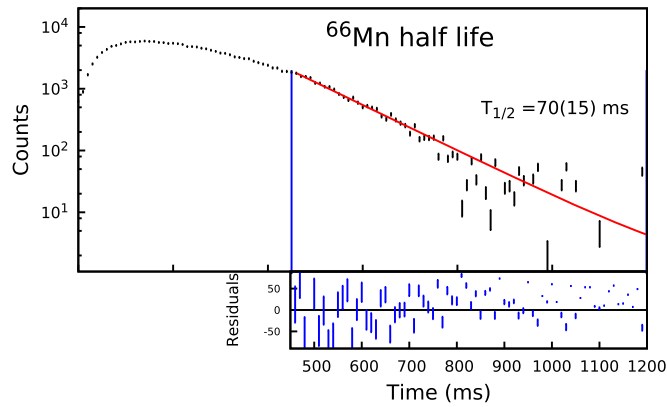
Figure 2. Activity curve of the 573.5 keV transition in ^{66}Fe, which corresponds to the ^{66}Mn decay half-life. The fit is done starting 450 ms after proton impact which is when the implantation is stopped. See text for details.
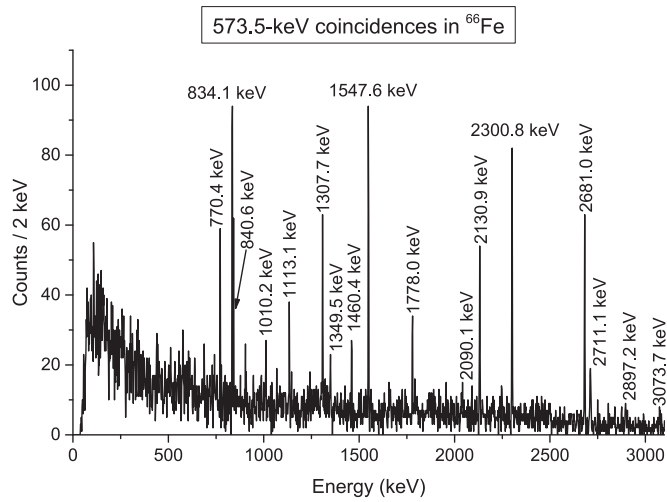

Figure 3. HPGe–HPGe coincidence energy spectrum with a gate on the 573.5 keV transition in ^{66}Fe.

short parent half-life, were assigned to the ^{66}Mn decay, although they could not be placed in the ^{66}Fe level scheme (see table 1).

The constructed level scheme for the β decay of ^{66}Mn to ^{66}Fe now includes a total of 16 levels and 24 γ transitions, as shown in figure 4. Details on the transitions, intensities and main coincidences are given in table 1. The relative intensities were obtained from the singles spectra (unless otherwise indicated) and normalized to 100 units for 573.5 keV. The intensities and energies of the γ rays that could not be unambiguously separated from other peaks in the singles spectra were obtained from $\gamma\gamma$ coincidences (see footnotes on table 1).

The transitions 1778.0 and 2130.9 keV, which were not placed in the level scheme reported in [23], have now been allocated. No transition at 2362.0 keV (reported with an absolute intensity of 2% in [23]) has been observed in this work, even if weaker transitions

Table 1. Summary of the observed transitions in the β decay of ^{66}Mn to ^{66}Fe. E_i stands for the parent level of the transition. The main coincident lines are given rounded up to the closest keV.

E_γ (keV)	I_γ	E_i (keV)	Coincident lines (keV)
573.5 (1)	100	573.5 (1)	770 834 841 1010 1133 1156 1308 1349 1460 1526 1548 1778 2090 2130 2246 2301 2681 2711 2897 3074
770.4 (1)	3.1 (2)	2891.4 (2)	573 1548
834.1 (1)[a]	8.8 (7)	1407.5 (1)	573 1156
840.6 (1)	6.2 (5)	1414.0 (1)	573 1460
1010.2 (2)	1.8 (2)	2891.4 (2)	573 1308 1881
1133.1 (2)	3.0 (2)	3254.4 (2)	573 1548
1156.2 (3)	0.8 (1)	2563.7 (3)	573 834
1307.7 (1)	6.1 (5)	1881.1 (1)	573 1010
1349.5 (2)	0.6 (1)	3470.6 (4)	573 1548
1460.4 (2)	2.8 (2)	2874.3 (1)	573 841
1526.3 (3)[a]	1.0 (1)	3647.2 (4)	573 1548
1547.6 (1)	13.2 (1)	2121.0 (1)	573 770 1133 1349 1526
1778.0 (1)	3.5 (3)	2351.5 (2)	573
1881.2 (1)	3.6 (3)	1881.1 (1)	1010
2090.1 (2)	1.6 (2)	2663.5 (1)	573
2130.9 (1)	8.4 (7)	2704.3 (1)	573
2245.8 (2)[a]	2.5 (7)	2819.3 (2)	573
2300.8 (1)	17 (1)	2874.3 (1)	573
2681.0 (2)	13 (1)	3254.4 (2)	573
2711.1 (2)	5.3 (5)	3284.6 (3)	573
2874.3 (1)	45 (4)	2874.3 (1)	—
2897.2 (4)	2.8 (3)	3470.6 (4)	573
3073.7 (5)	2.2 (2)	3647.2 (4)	573
3284.7 (2)	7.0 (1)	3284.6 (3)	—
4230.9 (4)[b]	1.5 (2)	—	—
5105.9 (3)[b]	0.4 (1)	—	—

[a] Intensity obtained from $\gamma-\gamma$ coincidences and normalized to the singles spectrum.
[b] Transitions assigned to the ^{66}Mn decay but not placed in the ^{66}Fe level scheme.

have been observed at similar energies. However a peak at 2363.3 keV was identified as the first escape peak of the intense 2874.3 keV transition. The authors of [23] also report a γ ray at 175.2 keV with an absolute intensity of 3.6(6)%, which is labeled as placed in the level scheme in their table 1, but it is not shown in their level scheme in figure 3. This transition was not observed in our experiment even if it should be well within the observation intensity limit. Finally we note that the level identified in our work at 2121.0 keV (see table 2) corresponds to the level mistakenly quoted at 2130 keV in [23], since the energies of the feeding and de-exciting transitions observed in [23] add up a value of 2121 keV.

The apparent β feeding to the levels was calculated as the intensity difference of the γ transitions feeding and de-populating a specific level. With a large decay window of $Q_\beta = 13.317(12)$ MeV (and $S_n = 6.918(8)$ MeV) [30] several unobserved high-energy transitions can be expected, and therefore the β feeding values should be taken as upper bounds. See table 2 for a list of levels, their deduced log(ft) and β feeding.

J. Phys. G: Nucl. Part. Phys. **44** (2017) 125103
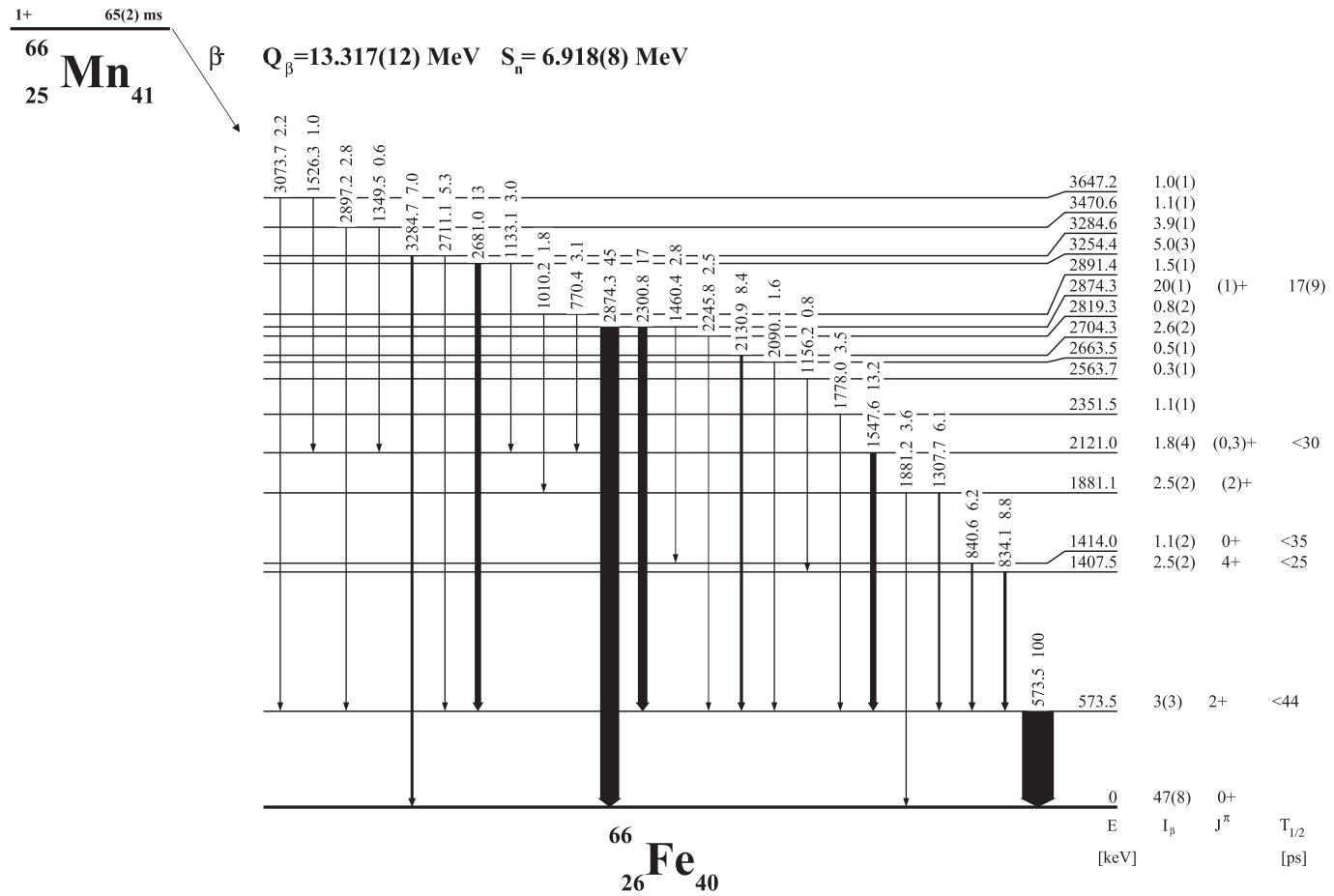
B Olaizola *et al*

7

Figure 4. ^{66}Fe level scheme populated in the β decay of ^{66}Mn from this work. The width of the transitions is proportional to their relative intensity. Some of the closely spaced levels have been displaced for a better visualization.
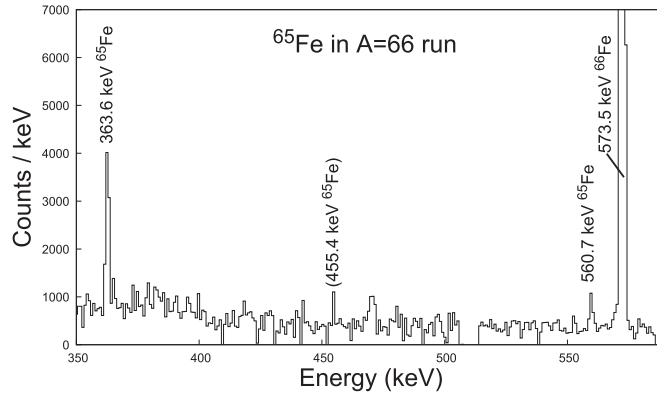
Figure 5. HPGe singles energy spectrum with a time window after proton impact on target that enhances the ^{66}Mn activity. The 363.7, and 560.8 keV, and the tentative 455.6 keV transitions were already observed in the ^{65}Mn β^- decay to ^{65}Fe [17]. In this case they have been assigned to the ^{66}Mn β–n branch.

Table 2. Summary of levels populated in the β decay of ^{66}Mn to ^{66}Fe, together with their apparent β-feeding, log(ft) value, measured half life and assigned spin-parity.

Energy (keV)	Beta-feeding (%)	Log(ft)	$T_{1/2}$ (ps)	J_π
g.s.	47(8)	5.1(1)		0^+
573.5(1)	3(3)	6.2(4)	<44	2^+
1407.5(1)	2.5(2)	6.13(4)	<25	4^+
1414.0(1)	1.1(2)	6.49(5)	<35	0^+
1881.1(1)	2.5(2)	6.05(4)		(2^+)
2121.0(1)	1.8(4)	6.15(10)	<30	$(0, 3)^+$
2351.5(2)	1.1(1)	6.32(10)		
2563.7(3)	0.3(1)	6.84(15)		
2663.5(1)	0.5(1)	6.6(1)		
2704.3(1)	2.6(2)	5.88(4)		
2819.3(2)	0.8(2)	6.4(1)		
2874.3(1)	20(1)	4.95(3)	17(9)	(1^+)
2891.4(2)	1.5(1)	6.08(4)		
3254.4(2)	5.0(4)	5.49(4)		
3284.6(3)	3.9(3)	5.59(4)		
3470.6(4)	1.1(1)	6.10(5)		
3647.2(4)	1.0(1)	6.10(5)		

2.2. β-delayed neutron emission branch

Figure 5 shows a HPGe spectrum where the 363.7 and 560.8 keV lines and possibly the 455.6 keV line, corresponding to transitions already known from the ^{65}Mn β^- decay to ^{65}Fe [17], are observed. These transitions have been assigned to the β–n branch in the ^{66}Mn decay and are observed for the first time in this work. Due to the lack of peak structure, the presence of a 455.6 keV transition is tentative. Since the ions were continuously deposited in an aluminium stopper data on the complete $A = 66$ and $A = 65$ decay chains populated through the β-decay of ^{66}Co was accumulated in saturation (no tape was removing the decay

Table 3. Summary of levels populated in the β–n decay of ^{66}Mn to ^{65}Fe and their observed de-exciting transitions. The γ ray intensities have been normalized to 100 units for 573.5 keV in ^{66}Fe.

E_{level} (keV)	β–n feeding (% from total)	Transition (keV)	Relative intensity
0.0	33(5)	—	—
363.7(1)	51(4)	363.7(1)	5.2(3)
455.6(2)[a]	7(3)	455.6(2)	0.7(2)
560.8(2)	9.3(11)	561.0(2)	1.0(1)

[a] The presence of this transition is tentative in the β–n branch.

products). The relative intensities of the members of the decay can be used to measure the β-delayed neutron emission probability. To obtain a reliable P_n value the ^{65}Fe decay to ^{65}Co was analyzed, where, for internal consistency, the absolute intensity of γ-rays in ^{65}Co measured in our data set were used [17]. The transitions at 1222.9 keV (13(1)% absolute intensity) and 1996.6 keV (23(2)%) were employed (the intense 882.1 keV transition in ^{65}Co could not be used because of the presence of the 881.5 keV line in ^{66}Co). Their intensities were compared to the observed 470.7 and 806.8 keV transitions in ^{66}Co with $I_{\text{abs}} = 15(3)\%$ and $I_{\text{abs}} = 5(2)\%$ respectively [31]. Their ratios yielded a value of $P_n = 3.9(8)\%$.

This value was further confirmed by analyzing the ^{65}Ni β^- decay to ^{65}Cu (the ^{65}Co to ^{65}Ni decay was not used because over 90% of the β decay directly populates the ground state [32]), where the intensity of the 1481.8 keV γ ray in ^{65}Cu, with absolute intensity of 23.6(2)%, was employed. Using only this transition a $P_n = 3.7(8)\%$ value was obtained, in excellent agreement with our previous result. As final result we take $P_n = 3.8(8)\%$ for the neutron-delayed branch of the ^{66}Mn decay. This value is in agreement with the recently published value of $P_n = 4(1)\%$ [23]. In table 3 the β–n feeding of the levels has been normalized to add up to 100% for the whole β–n branch. The direct feeding to the ground state, calculated as the excess of intensity in the observed ^{65}Co transitions, amounts to 33(5)% of the total β–n branch.

2.3. Direct β feeding to the ground state

The direct ^{66}Mn β feeding to the ^{66}Fe ground state was estimated from the observed γ-intensity balance of the different isotopes of the decay chain. For this purpose we compare the intensity of the 573.5 keV line γ-ray in ^{66}Fe with intense transitions in the ^{66}Co daughter, whose absolute intensity is taken from the literature [31]. The intensity of the 573.5 keV γ ray in ^{66}Fe represents 64(5)% of the total γ intensity populating the ^{66}Fe ground state. The 470.7 and 806.8 keV transitions in ^{66}Co, show relative intensities of $I_{\text{rel}} = 46(1)$ and $I_{\text{rel}} = 15(1)$ referred to the 573.5 keV transition in ^{66}Fe normalized to $I_{\text{rel}} = 100$. When corrected for their absolute intensities, $I_{\text{abs}} = 15(3)\%$ and $I_{\text{abs}} = 5(2)\%$ respectively [31], they show an excess of intensity. This excess was atributed to direct β feeding of the ^{66}Fe ground state. The analysis from these γ rays gave results in great agreement, and the average, after the correction for the β–n branch (see previous section), yields a direct ^{66}Mn β feeding to the ^{66}Fe ground state of 47(8)%. The main source of error in this value are the uncertainties of the ^{66}Co total intensities. The value is larger but in agreement with the published value of 36(6)% [23]. Our result relies on the published absolute intentisties for γ-rays in ^{66}Co following the ^{66}Fe decay, and will be strongly affected if these change, in particular if more ground state transitions are found.

We tried to verify this result by comparing the decay of ^{66}Co into ^{66}Ni, but the measured absolute intensities from our work were found to be lower by a factor of 5 or more than those available in the literature [33]. At the time of the study reported in [33] a (3^+) spin had tentatively been assigned to the ^{66}Co ground state [34], whereas a more recent publication suggests (1^+) [31]. This new spin would imply a strong direct β feeding to the 0^+ ground state in the even–even ^{66}Ni, which would explain the large discrepancy in absolute intensities by the missed ground-state feeding. Therefore this decay cannot be used to cross check the direct β-feeding to the ^{66}Fe ground state.

3. Fast-timing analysis

Level lifetimes in ^{66}Fe were measured using the ATD $\beta\gamma\gamma(t)$ method [24–26]. The centroid shift technique was employed to determine the half-life of the 573.5 keV level in $\beta\gamma\gamma$ coincidences. For this purpose the 834.1 keV $-$ 573.5 keV γ cascade was used. Two time-difference distributions between β particles and γ-rays detected in the LaBr$_3$(Ce) detectors were obtained with time-to-amplitude converter analog modules. One of the distributions required the selection of the the 834.1 keV in the HPGe and the 573.5 keV in the LaBr$_3$(Ce) detectors, while the second one was obtained by reversing the gates. The difference between the two time distributions, corrected by Compton contributions under full-energy peaks (FEPs) and by the time walk as a function of energy for FEPs (given by the approximate prompt curve, APC [24]) yields the 573.5 keV state lifetime. The result is $\tau = 46(33)$ ps, correspoding to $T_{1/2} = 32(23)$ ps, which is in agreemenet with previous direct measurements [11, 12], but with a very large error bar due to the limited statistics for this analysis.

A second measurement of the half-life of the 573.5 keV level was performed using $\beta\gamma$ coincidences. This requires an absolute prompt ($\tau \sim 0$ ps) reference to shift the measured time centroids to the APC. For the $A = 66$ run there was no suitable candidate found within the ^{66}Mn decay, so a transition from a different nucleus measured in the same data set was used instead. The most intense γ-ray in the ^{66}Ga decay to ^{66}Zn is the 1039.2 keV transition, which de-excites the 2_1^+ 1039.2 keV state. This state has a $T_{1/2} = 1.68(3)$ ps, which has been obtained as the weighted average of over 10 different experiments [29]. This combination of a short and precise half-life with high intensity makes this transition a candidate for the absolute prompt reference calibration. Thanks to the careful calibration of the time-walk for the plastic scintillator detecting the β-particles, the systematic error introduced by ^{66}Ga decaying via β^+/EC and with a different Q_β window of 5175(3) keV [29] was minimized to a few ps level, the sensitivity of the method. Using this transition, the shift to the APC at 1039.2 keV has been measured independently for the two LaBr$_3$(Ce) detectors, using the time difference betwen β particles and 573.5 keV photons in $\beta\gamma$ coincidences, as shown in figure 6. One of the fast detectors yielded a lifetime of $\tau_1 = 46(19)$ ps while the other $\tau_2 = 53(18)$ ps. These values suffer from the unknown (although small) contribution due to feeding from higher-lying levels, and therefore the result provides an upper limit for the 2^+ lifetime, yielding $\tau < 63$ ps. The reduced transition rate for the E2 573.5 keV transition is larger than 190 e^2 fm^2, equivalent to B(E2;$2_1^+ \to 0_1^+$) > 12 W.u., see table 4. The result is consistent with the analysis using $\beta\gamma\gamma$ coincidences and with previously reported values obtained by different experimental methods [11, 12], as plotted in figure 8.

The 834.1 and 840.6 keV transitions cannot be resolved in the LaBr$_3$(Ce) energy spectra, and therefore the time difference between β and γ events when the double peak 834.1/ 840.6 keV is selected gives a time distribution shifted by the intensity-weighted average of both mean lives. When shifted to the APC this time distribution yields an upper limit of
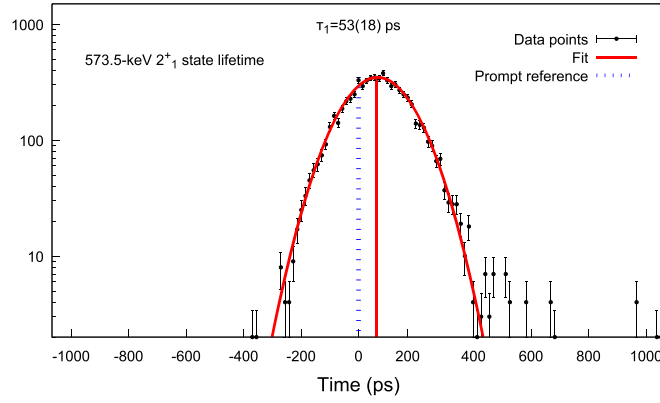
Figure 6. Time difference of $\beta\gamma$ coincidences with a gate on the 573.5 keV peak for one of the LaBr$_3$(Ce) detectors. Its centroid shift from the prompt curve is due to the mean life of the 2_1^+ state and small contributions from high-lying states. See text for details.

Table 4. Transition rates obtained in the timing analysis. For the assigned multipolarity to the transitions (column *Mult. Xλ*) the experimental transition rates (column $B(X\lambda)_{\text{exp}}$) and the calculated ones ($B(X\lambda)_{\text{theo}}$) are given in W.u.

E_{level} (keV)	$T_{1/2}$ (ps)	E_γ (keV)	$J_i^\pi \to J_f^\pi$	Mult. ($X\lambda$)	$B(X\lambda)_{\text{exp}}$ (W.u.)	$B(X\lambda)_{\text{theo}}$ (W.u.)
573.5(1)	<44	573.5(1)	$2^+ \to 0^+$	E2	>12[a]	18
1407.5(1)	<25	834.1(1)	$4^+ \to 2^+$	E2	>3.5	27
1414.0(1)	<35	840.6(1)	$0^+ \to 2^+$	E2	>2.4	0.36
2121.0(1)	<30	1547.6(1)	$(0, 3)^+ \to 2^+$	M1	>1.9 × 10^{-4}	
				E2	>0.13	
2874.3(1)	17(9)	1460.4(2)	$1^+ \to 0^+$	M1	1.8(9) × 10^{-5}	0.06
		2300.8(1)	$1^+ \to 2^+$	M1	2.8(15) × 10^{-5}	0.11
		2874.3(1)	$1^+ \to 0^+$	M1	3.8(20) × 10^{-5}	0.11

[a] The triple $\beta\gamma\gamma(t)$ coincidence measurement yields 15(11) W.u.

$T_{1/2} < 15$ ps. Assuming a half-life of $\tau \sim 0$ ps for the 0_2^+ state, an upper limit of $T_{1/2} < 25$ ps can be set for the 4_1^+ state. On the other hand, if we assume that the 4_1^+ level is the one with a prompt half-life we can a set an upper limit of <35 ps to the 0_2^+ state. These conservative upper limits have been included in table 4.

The half-life of the 2874.3 keV level was measured using the 2874.3 keV transition in $\beta\gamma$ coincidences ($T_{1/2} = 17(9)$ ps, see table 4). This result was independently confirmed in triple coincidences by gating on the 2300.8 keV transition in the LaBr$_3$(Ce) crystals and setting an extra gate in the 574 keV peak in the HPGe, which yielded an upper limit of <30 ps. In this case no contribution from higher-lying states can be expected. In a similar way the half life of the 2121.0 keV level was measured using the 1547.6 keV transition, which yielded a $T_{1/2} < 30$ ps limit.

The reduced transition probabilities have been extracted from the measured half lives and the branching ratios, see table 4.

4. Shell-model calculations

To help characterize the ^{66}Fe nuclear structure, we have performed shell-model calculations using the LNPS effective interaction [20]. In the calculations ^{48}Ca is taken as a closed core. The valence space includes the complete *pf* shell for the protons and the $0f_{5/2}$, $1p_{3/2}$, $1p_{1/2}$, $0g_{9/2}$, and $1d_{5/2}$ orbitals for the neutrons.

The calculation proceeds as follows: first the (1^+) ^{66}Mn state (tentatively assigned to be the ground state in [35]) is calculated. Notice, however, that the calculation produces a bunch of closely packed states among which the 1^+ is not the lowest; as we shall discuss later, this state has higher particle–hole rank than its neighbors, therefore, it could well gain more energy than the other states would, if we were able to perform calculations in a even larger space. Then we act on the (1^+) ^{66}Mn state with the Gamow–Teller operator and use the Lanczos technique to get the corresponding strength function, from which we obtain the energies of the levels fed by the β-decay and their $\log(ft)$ values. Only allowed transitions are enabled and therefore only 0^+, 1^+ and 2^+ states in ^{66}Fe are populated. Levels in the ^{66}Fe daughter up to an excitation energy of 4 MeV have been calculated. In addition, other positive-parity levels with spin up to 4^+ have been directly calculated in ^{66}Fe. No negative-parity states are computed. The calculations are carried out at a level of truncation $t = 8$, i.e. up to eight particles can be excited across $N = 40$ and/or $Z = 28$. With the resulting wave functions we compute the occupancies of the spherical orbits and the reduced E2 and M1 transition probabilities between the states, thus allowing the comparison to the experimental values. We use effective E2 charges 0.46 and 1.31 for neutrons and protons, respectively, and effective gyromagnetic factors, $g_s = 0.75\, g_s^{\text{bare}}$, $g_l^{\pi} = 1.1$, and $g_l^{\nu} = -0.1$. Standard quenching $q = 0.75$ is applied to the Gamow–Teller decays. Figure 7 shows a comparison of the shell-model levels with the experimental energies.

Table 5 shows the levels obtained in the calculations, their $\log(ft)$ and their proton and neutron occupation numbers for the $\nu(1p_{3/2}$, $0f_{5/2}$, $1p_{1/2}$, $0g_{9/2}$, $1d_{5/2})$ and $\pi(0f_{7/2}$, $1p_{3/2}$, $0f_{5/2}$, $1p_{1/2})$ orbitals. A characteristic feature of most ^{66}Fe states is their large occupancies of the neutron $0g_{9/2}$ and $1d_{5/2}$ orbitals. As seen from table 5, the $0g_{9/2}$ orbital plays a dominant role with most of the levels showing an average neutron occupation in excess of 3. The inclusion of the higher-lying $1d_{5/2}$ is duly justified as seen from its occupancy in the calculated levels. Notice also the important role of the proton excitations across $Z = 28$ (0.8 on average). As discussed in detail in [36] both neutron and proton excitations are necessary to make ^{66}Fe deformed. Table 4 shows calculated M1 and E2 transition rates, where the transition energies have been obtained as the difference of the level energies.

Figure 8 shows a comparison of the different calculated B(E2; $2_1^+ \rightarrow 0_1^+$) values. The difference with the results shown in [12] is due to the different effective charges employed and, in fact, the theoretical B(E2) values of [11] should be preferred to the present ones because they were obtained at a better ($t = 12$) truncation level, which is computationally out of reach for the detailed calculation of the β decay of ^{66}Mn presented for the first time in this article. Nevertheless the difference between both sets of calculations is of the order of $\sim$5%.

Another recent shell-model calculation [37], using an effective interaction derived from the CD-Bonn nucleon–nucleon potential, obtains results in good agreement with ours, even if they use a smaller proton valence space, which does not include the $0f_{5/2}$ and $1p_{1/2}$ orbits. This choice may be questionable, given the nearly equal occupancies of the $0f_{5/2}$ and $1p_{3/2}$ orbits (see table 5). Nevertheless, it predicts neutron occupancies for the ground state similar to ours and a $\sim$25% smaller B(E2; $2_1^+ \rightarrow 0_1^+$) transition rate for ^{66}Fe (see figure 8).
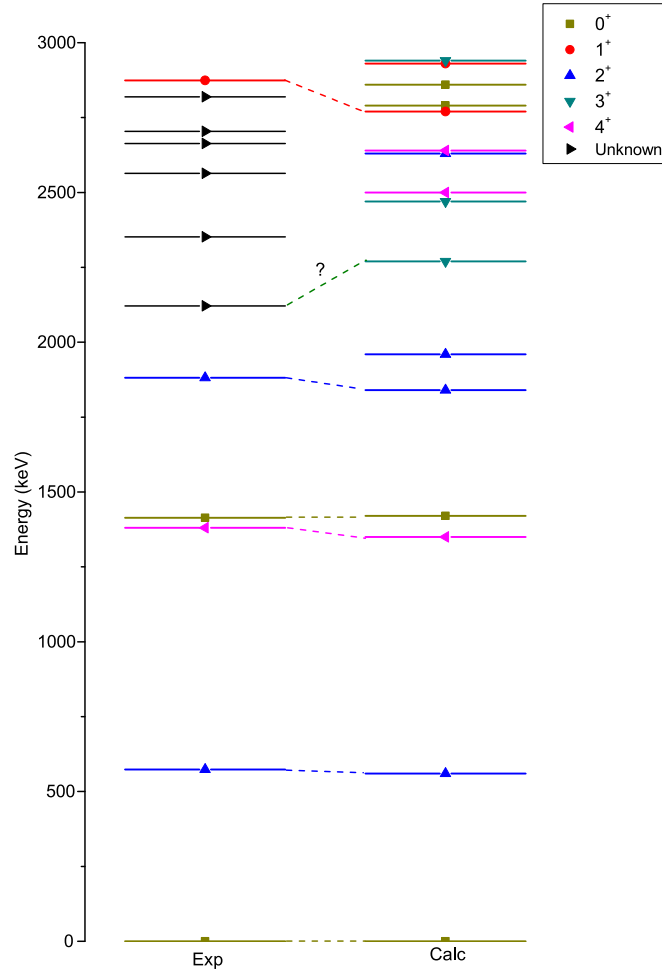
Figure 7. Comparison of the shell-model calculations and the experimental level scheme. The calculated values include positive parity levels up to 4^+. See text for details. The experimental 4_1^+ state has been shifted down in energy for a better visualization.

Our calculations also show that the ^{66}Fe ground, 2_1^+ and 4_1^+ states are dominated by neutron configurations of high particle–hole rank. Therefore, it is the inversion of the normal and intruder states which governs the physics of this nucleus, and gives rise to a deformed yrast band. This deformed ground state interpretation is in agreement with the calculations presented in [36], in which the authors employed different methods to calculate deformation and orbital occupation numbers for $N = 40$ isotones. While this deformation interpretation is supported by the experimental data presented (lowering of the E(2_1^+) and large B(E2) value) and by our shell-model calculations, IBM-2 calculations predicts a different behavior for the quadrupole moment and the energy ratio, suggesting a more complex structure [38]. Shape coexistence was predicted in the region by Carpenter *et al* [7], but they proposed a dominant spherical ground state and a deformed excited band. The calculations from our work discard this scenario.

J. Phys. G: Nucl. Part. Phys. **44** (2017) 125103

B Olaizola *et al*

14

Table 5. Calculated ^{66}Fe levels in the valence space $\nu(1p_{3/2}\ 0f_{5/2},\ 1p_{1/2}, 0g_{9/2},\ 1d_{5/2})$ and $\pi(0f_{7/2},\ 1p_{3/2}, 0f_{5/2},\ 1p_{1/2})$, and log$ft$ values for the decay of the 1^+ state of ^{66}Mn. The proton and neutron occupation columns list the average occupation numbers of the valence orbitals. The occupation in the mother nucleus ^{66}Mn are displayed as well. When a reliable identification of states has been possible, the experimental energies and log(ft) have been included for comparison.

^{66}Mn					Proton occupation				Neutron occupation				
E(keV)		J^π			$f_{7/2}$	$p_{3/2}$	$f_{5/2}$	$p_{1/2}$	$p_{3/2}$	$f_{5/2}$	$p_{1/2}$	$g_{9/2}$	$d_{5/2}$
g.s.		1^+			3.4	0.6	0.6	0.4	4	3.7	1.2	3.3	0.8
^{66}Fe					Proton occupation				Neutron occupation				
E_{th}(keV)	$\log(ft)_{\mathrm{th}}$	J^π	E_{exp}(keV)	$\log(ft)_{\mathrm{exp}}$	$f_{7/2}$	$p_{3/2}$	$f_{5/2}$	$p_{1/2}$	$p_{3/2}$	$f_{5/2}$	$p_{1/2}$	$g_{9/2}$	$d_{5/2}$
0	6.35	0^+	0	5.1(1)	5.2	0.4	0.3	0.1	3.9	3.7	0.9	3.1	0.4
0.56	5.94	2^+	573.5(1)	6.2(4)	5.1	0.4	0.3	0.2	3.9	3.6	0.7	3.3	0.5
1.35		4^+	1407.5(1)	6.13(4)	5	0.5	0.3	0.2	3.9	3.6	0.6	3.4	0.5
1.42	7.32	0^+	1414.0(1)	6.49(5)	5.2	0.4	0.3	0.1	3.9	4	1.3	2.4	0.4
1.84	6.72	2^+	1881.1(1)	6.05(4)	5.1	0.4	0.3	0.2	3.9	3.6	0.7	3.3	0.5
1.96	>8	2^+			5.1	0.4	0.3	0.2	3.9	3.8	1.3	2.6	0.4
2.27		3^+	2121.0(1)[a]	6.15(10)	4.5	0.6	0.5	0.4	3.9	3.5	0.7	3.3	0.6
2.47		3^+											
2.5		4^+			4.5	0.5	0.6	0.4	3.9	3.5	0.7	3.3	0.6
2.63	6.52	2^+			5.2	0.4	0.3	0.1	3.9	3.9	1.3	2.6	0.3
2.64		4^+											
2.77	6.4	1^+	2874.3(1)	4.95(3)	5	0.4	0.4	0.2	3.9	3.4	0.9	3.3	0.5
2.79	7.8	0^+			4	0.6	0.8	0.6	3.9	3.7	0.7	3.1	0.6
2.86	6.26	0^+											
2.93	7.17	2^+											
2.94		3^+											
3.04	7.8	1^+											
3.49	5.55	0^+											
3.92	6.34	1^+											

[a] The assignment of the 2121.0 keV level as the 3_1^+ is less firm than in the other cases, see text for details.
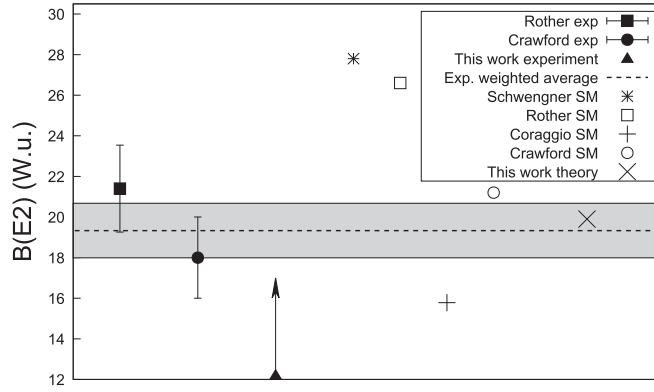
Figure 8. Comparison of the experimental ([11, 12] and this work) and calculated ([11, 12, 37, 39] and this work) B(E2; $2^+ \rightarrow 0^+$) reduced transition probability. The dashed line is the weighted average of the three experimental values and the gray band its uncertainty. The authors of [12] took effective charges 0.5 and 1.5 which was an standard choice at that time. We now favor the microscopically derived ones (0.46, 1.31) [40], when the core has a doubly magic closure in the armonic oscillator or a very stiff one as in ^{48}Ca. The theoretical results of [12] have been recalculated with the present effective charges, which were also used in [11]. In [37], the effective charges are orbit dependent at variance with the other SM calculations.

Our results are also in contrast with the shell-model calculation presented in [23]. In their work the authors predicted the excitation of about 1.2 protons above the $Z = 28$ closure and, on average, only two neutrons to the $0g_{9/2}$ orbital, compared with our 0.6 protons and three neutrons. They also predicted a 0_2^+ excited state with a closed shell at $\sim$1.7 MeV. These differences can be explained by the inclusion of the $\nu 1d_{5/2}$ orbital in our calculations, while in the ones presented in [23] the neutron model space did not incorporate it. Notice as well the mismatch between the occupancies of the parent nucleus ^{66}Mn and most of the the states fed in ^{66}Fe, whence the rather low calculated log(ft) values.

5. Discussion

Using the obtained experimental information for the energy levels and the transition rates, and with the guidance of the theoretical calculations, we have insight into the ^{66}Fe nuclear structure.

Ground state, $J^\pi = 0^+$: A high direct β-feeding to the ground state was obtained in our experiment; this would confirm the tentative assignment of (1^+) for the ^{66}Mn ground state [35], but our observation is largely based on the existing experimental information on the decay of ^{66}Fe to ^{66}Co [31]. According to the calculations, the dominant configuration of the $\{f_{5/2}\ p_{1/2}\ g_{9/2}\ d_{5/2}\}$ neutron orbitals is an admixture of $\{4220\}$ and $\{4040\}$, thus 2 holes in the *fp* shell and 2 particles in $0g_{9/2}$ (2p2h) and 4 holes–4 particles (4p4h). The excitation of 3 neutrons on average to the $0g_{9/2}$–$1d_{5/2}$ orbits shows that the intruder configurations drop below the normal ones, driving the nucleus ^{66}Fe into the deformed regime.

573.5 keV, $J^\pi = 2^+$: Its configuration is the same as that of the ground state, an admixture of (2p2h) and (4p4h). Our level half-life limit $T_{1/2} < 44$ ps yields a reduced transition probability to the ground state of B(E2) > 12 W.u., which can be compared to the

value B(E2) = 21(2) W.u. in [12] or the B(E2) = 18(2) W.u. in [11]. This is in good agreement with the calculated rate of B(E2) = 20 W.u., see figure 8.

The calculation suggests a small direct β-feeding to this level, with $\log(ft) = 5.94$, in agreement, within error bars, with the observed apparent $\log(ft)$ in the experiment.

2874.3 keV, $J^\pi = (1^+)$: This level has a direct β-feeding of 20(1)% and the lowest log (ft) of the present level scheme, which suggests an allowed transition from the (1^+) parent g.s. and thus 0^+, 1^+ or 2^+ spin-parity. The intense transition to the 0^+ ground state rules out the 0^+ option. If it had 2^+ spin-parity it should de-excite to both the 0_2^+ and the 4_1^+ levels around 1.4 MeV (see following paragraphs) with similar intensity, while it only clearly populates one of them. If 1^+ spin-parity is assigned, it would only populate the 0_2^+ level at $\sim$1.4 MeV, while there should be no observable transition to the 4^+. Thus 1^+ seems to be the most likely assignment for the spin-parity of the 2874.3 keV state. In our shell-model calculations the first 1_1^+ state is obtained at 2.77 MeV, in remarkably good agreement with the measured energy.

In the experiment we have measured a half-life of 17(9) ps for this level at 2874.3 keV. With this half-life the transition probabilities are low for both M1 and E2, but none of them can be discarded and neither the 1^+ nor the 2^+ assignment for the level can be completely ruled out.

1407.5 keV, $J^\pi = (4^+)$: Reaction experiments tentatively assign spin 4^+ to a level at 1407 (6) keV [10, 22]. In our experiment this level populates the 2_1^+ but not the 0^+ ground state and is not populated by the the 1_1^+ at 2874.3 keV, which suggests a spin of 3^+ or higher. We have set an upper limit of 25 ps for the half-life of this level. The resulting transition rates B(E2) > 3.5 W.u. and B(M1) > 1.5×10^{-3} W.u. do not allow us to characterize the multipolarity of the transition, since both are within the systematics. But our calculations suggests that the 4_1^+ state is around 1.35 MeV, while the 3_1^+ is over 2.2 MeV, so we support the previous assignment of 4_1^+ for this level. Being the β decay forbidden, its apparent β feeding may be explained by high-energy γ rays not observed in this experiment.

1414.0 keV, $J^\pi = (0^+)$: This level only populates the 2_1^+ and is populated from the 1_1^+ level. A spin of 3 or lower is thus expected, but if the spin were 1^+ or 2^+ a strong population to the 0^+ ground state should be observed, which is not the case. As mentioned above, the calculations do not obtain a level with spin 3^+ up to 2.27 MeV, and thus we assign 0^+ as the most likely spin-parity. The calculations give a 0_2^+ state at 1.42 MeV, in excellent agreement with this assignment. The measured upper limit of $T_{1/2} < 35$ ps does not help deduce the multipolarity of the transition, since B(E2) > 2.4 W.u. and B(M1) > 1.1×10^{-3} W.u. are reasonable rate limits. The calculation predicts a value of $B(0_2^+ \rightarrow 2_1^+) = 9.0$ W.u., in agreement with the identification of this level as being the 0_2^+ state.

1881.1 keV, $J^\pi = (2^+)$: In the calculations the second and third 2^+ states appear at 1.84 and 1.96 MeV, respectively. The 1881.1 keV level has two transitions to the 0_1^+ and the 2_1^+ states, but there are no observed transitions to the 1407.5 and 1414.0 keV levels (of spin (4^+) and (0^+), respectively). If 2^+ spin is assigned to this level, the unobserved transitions would be E2 in character and their intensity would be less than 0.1, below the experimental detection limit. The calculations predict a 993.2 keV M1 transition from the 1_1^+ state at $\sim$2.8 MeV to the 2_2^+ level with a B(M1) of around 1/2 of that of the $1_1^+ \rightarrow 2_1^+$ 2300.8 keV transition and of almost the same strength to the 2_3^+ state. This 993.2 keV transition would have a relative intensity of $\sim$0.05 in the first case or assuming similar B(M1) for the 993.2 and 2300.8 keV $\sim$0.25, in either case far from our detection limit.

2121.0 keV, $J^{\pi} = (0, 3^+)$: This level only feeds the 2_1^+ state and is fed by several higher energy levels. If 2^+ spin-parity was assigned to this level, an intense E2 transition of 2121.0 keV to the ground state should be observed, so this option can be rejected. On the other hand, if we assume that this level has 3^+ spin-parity, it would explain why it does not populate the 0^+ states below it, but a transition of 713.5 keV to the 1407.5 keV 4_1^+ with a relative intensity of the order of 1 would be missing. Since this intensity is very close to the detection limit, the 3^+ spin can not be ruled out. With a similar argument, 0^+ spin can be assigned to this level. It would explain why it does not populate the ground state or the 0_2^+ and the 4_1^+, while the transition from the 1^+ would have a relative intensity below 0.5, which explains why it is not observed.

The calculations predict the 3_1^+ at 2.27 MeV and the next 0_3^+ at 2.79 MeV, so the 3^+ assignment seems more likely. Why the high-energy levels favors the population of this level over lower ones remains unexplained. The lifetime upper limit of <30 ps does not help to distinguish if the 1547.6 keV transition is of M1 or E2 character, as both limits are reasonable. In the case of the M1 character it would be faster than other M1 transitions in this nucleus. This feature is also present in the calculations (see table 4).

Higher-lying states: In the energy range from 2.3 to 3.0 MeV seven levels have been identified experimentally, including the 2874.3 keV discussed above. Following the comparison, tentative assignments of $J^{\pi} = (3, 4)^+$ could be made for the 2351.5 keV and 2663.5 keV levels and, based on the larger apparent β-feeding, the 2704.3 keV state could tentatively be the 0_3^+ obtained in the calculations at 2.86 MeV.

Concerning the 3284.6 keV level, strong feeding to the low-lying 0_1^+ and 2_1^+ states is observed, so $J^{\pi} = (1, 2)^+$ are possible options. The calculation shows a 2^+ at 2.9 MeV and a 1^+ at 3.0 MeV, in reasonable agreement for this energy range.

No negative parity states have been considered for this level scheme, since they are expected to appear at higher energies and have negligible feeding. For reference, in ^{64}Fe the lowest negative parity state found up to date has $(5)^-$ spin-parity and it is located at 2.8 MeV [41].

6. Conclusions

The ^{66}Fe level scheme constructed in this work confirms most of the γ rays previously observed and expands it to include a total of 24 transitions and 16 excited levels. Two other high-energy γ rays were assigned to the ^{66}Mn decay, but could not be unambiguously placed on the level scheme. The observed direct β-feeding to the ground state of 47(8)% is in agreement with the literature. An improved value of $P_n = 3.8(8)$% has been obtained for the neutron delayed emission branch. Moreover, population to excited states in ^{65}Fe has been observed for the first time.

Employing the ATD $\beta\gamma\gamma(t)$ method, specifically the centroid shift technique, the half-life of the 2874.3 keV state has been measured and upper limits have been established for four levels. The measured half-life limit for the 2_1^+ state and the experimental transition rate B(E2; $2_1^+ \rightarrow 0_1^+$) > 12 W.u. are in agreement with previously reported values and indicate a high collectivity in this nucleus.

Extensive shell-model calculations using the LNPS effective interaction have been performed, providing information on the ^{66}Mn β decay and the ^{66}Fe nuclear structure. Our calculations support the multineutron particle–hole character of most of the states in ^{66}Fe. They are also able to reproduce the energy of the 2_1^+ state state and the B(E2) transition rate to the ground state. Making use of the experimental level scheme and the deduced transition

rates, and with the comparison to the shell-model calculations, spin-parity has been proposed for several levels. We confirm the previous tentative identification of the 4_1^+ state and propose the assignment of the 1_1^+ at 2874.3 keV, based on the experimental information and on the shell-model calculations, available for the first time for the 1^+ states.

Acknowledgments

ORCID iDs

B Olaizola ⬤ https://orcid.org/0000-0003-1604-0640
L M Fraile ⬤ https://orcid.org/0000-0002-6281-3635
A Poves ⬤ https://orcid.org/0000-0001-7539-388X

References

[1] Broda R *et al* 1995 *Phys. Rev. Lett.* **74** 868–71
[2] Sorlin O *et al* 2002 *Phys. Rev. Lett.* **88** 092501
[3] Guénaut C *et al* 2007 *Phys. Rev.* C **75** 044303
[4] Tsunoda Y, Otsuka T, Shimizu N, Honma M and Utsuno Y 2013 *J. Phys.: Conf. Ser.* **445** 012028
[5] Recchia F *et al* 2013 *Phys. Rev.* C **88** 041302
[6] Flavigny F *et al* 2015 *Phys. Rev.* C **91** 034310
[7] Carpenter M P, Janssens R V F and Zhu S 2013 *Phys. Rev.* C **87** 041305
[8] Crider B *et al* 2016 *Phys. Lett.* B **763** 108–13
[9] Hannawald M *et al* (The ISOLDE Collaboration) 1999 *Phys. Rev. Lett.* **82** 1391–4
[10] Adrich P *et al* 2008 *Phys. Rev.* C **77** 054306
[11] Crawford H L *et al* 2013 *Phys. Rev. Lett.* **110** 242701
[12] Rother W *et al* 2011 *Phys. Rev. Lett.* **106** 022502
[13] Gade A *et al* 2010 *Phys. Rev.* C **81** 051304(R)
[14] Zuker A P, Retamosa J, Poves A and Caurier E 1995 *Phys. Rev.* C **52** R1741–5
[15] Radulov D *et al* 2013 *Phys. Rev.* C **88** 014307
[16] Lunardi S *et al* 2007 *Phys. Rev.* C **76** 034303
[17] Olaizola B *et al* 2013 *Phys. Rev.* C **88** 044306
[18] Olaizola B *et al* 2015 *JPS Conf. Proc.* **6** 030006
[19] Otsuka T, Suzuki T, Fujimoto R, Grawe H and Akaishi Y 2005 *Phys. Rev. Lett.* **95** 232502
[20] Lenzi S M, Nowacki F, Poves A and Sieja K 2010 *Phys. Rev.* C **82** 054301
[21] Ljungvall J *et al* 2010 *Phys. Rev.* C **81** 061301
[22] Fioretto E *et al* (The PRISMA and CLARA collaborations) 2010 *J. Phys.: Conf. Ser.* **205** 012038
[23] Liddick S N *et al* 2013 *Phys. Rev.* C **87** 014325
[24] Mach H, Gill R and Moszyński M 1989 *Nucl. Instrum. Methods Phys. Res.* A **280** 49–72
[25] Moszyński M and Mach H 1989 *Nucl. Instrum. Methods Phys. Res.* A **277** 407–17
[26] Mach H, Wohn F, Molnár G, Sistemich K, Hill J C, Moszyński M, Gill R, Krips W and Brenner D 1991 *Nucl. Phys.* A **523** 197–227

[27] Olaizola B 2013 Ultra-fast timing study of exotic neutron-rich isotopes *PhD Thesis* Universidad Complutense de Madrid, España (http://eprints.ucm.es/24121/1/T350)
[28] Olaizola B *et al* 2017 *Phys. Rev.* C **95** 061303
[29] Browne E and Tuli J 2010 *Nucl. Data Sheets* **111** 1093–209
[30] Naimi S *et al* 2012 *Phys. Rev.* C **86** 014325
[31] Liddick S N *et al* 2012 *Phys. Rev.* C **85** 014328
[32] Pauwels D *et al* 2009 *Phys. Rev.* C **79** 044309
[33] Mueller W F *et al* 2000 *Phys. Rev.* C **61** 054308
[34] Bosch U *et al* 1988 *Nucl. Phys.* A **477** 89–104
[35] Liddick S N *et al* 2011 *Phys. Rev.* C **84** 061305
[36] Rodríguez T R, Poves A and Nowacki F 2016 *Phys. Rev.* C **93** 054316
[37] Coraggio L, Covello A, Gargano A and Itaco N 2014 *Phys. Rev.* C **89** 024319
[38] Kotila J and Lenzi S M 2014 *Phys. Rev.* C **89** 064304
[39] Schwengner R, Frauendorf S and Brown B A 2017 *Phys. Rev. Lett.* **118** 092502
[40] Dufour M and Zuker A P 1996 *Phys. Rev.* C **54** 1641–60
[41] Hoteling N *et al* 2006 *Phys. Rev.* C **74** 064313